

Provided for non-commercial research and education use.  
Not for reproduction, distribution or commercial use.



(This is a sample cover image for this issue. The actual cover is not yet available at this time.)

This article appeared in a journal published by Elsevier. The attached copy is furnished to the author for internal non-commercial research and education use, including for instruction at the authors institution and sharing with colleagues.

Other uses, including reproduction and distribution, or selling or licensing copies, or posting to personal, institutional or third party websites are prohibited.

In most cases authors are permitted to post their version of the article (e.g. in Word or Tex form) to their personal website or institutional repository. Authors requiring further information regarding Elsevier's archiving and manuscript policies are encouraged to visit:

<http://www.elsevier.com/copyright>



Contents lists available at SciVerse ScienceDirect

## Journal of Alloys and Compounds

journal homepage: [www.elsevier.com/locate/jalcom](http://www.elsevier.com/locate/jalcom)

# Modification of the optoelectronic properties of sprayed $\text{In}_2\text{S}_3$ thin films by indium diffusion for application as buffer layer in CZTS based solar cell

V.G. Rajeshmon, N. Poornima, C. Sudha Kartha, K.P. Vijayakumar\*

Department of Physics, Cochin University of Science and Technology, Cochin 682 022, India

## ARTICLE INFO

## Article history:

Received 6 August 2012

Received in revised form 10 November 2012

Accepted 12 November 2012

Available online 27 November 2012

## Keywords:

Spray pyrolysis

Indium sulfide

CZTS

Solar cell

Buffer layer

## ABSTRACT

In this report the authors discuss the effect of diffusion of metallic indium on the optoelectronic properties of chemical spray deposited indium sulfide ( $\text{In}_2\text{S}_3$ ) thin films which are prospective candidates for buffer layer application in thin film solar cells. Thin layers of metallic indium having different thicknesses were diffused into the films by evaporating different quantities of indium using vacuum evaporation technique followed by annealing. 'In' diffusion was done with an aim to reduce resistivity and improve the crystallinity to ensure better carrier collection. X-ray diffraction, X-ray photoelectron spectroscopy, optical absorption, photoluminescence and electrical studies were performed on the films. Analysis indicated that crystallinity attained a maximum for an optimum 'In' diffusion and then showed a retracing nature. Resistivity was found to decrease drastically from  $2.3 \times 10^5 \Omega \text{ cm}$  [pristine] to  $4.7 \Omega \text{ cm}$  [for the optimum indium diffused samples]. Using the optimized  $\text{In}_2\text{S}_3$  layer and copper zinc tin sulfide (CZTS) deposited using chemical spray pyrolysis, a heterojunction device was successfully fabricated with a conversion efficiency of 1.85% and fill factor of 52%. The optimum quantity of indium to be diffused depends on the thickness of the  $\text{In}_2\text{S}_3$  thin film.

© 2012 Elsevier B.V. All rights reserved.

## 1. Introduction

Recently, there has been an increasing interest in III–VI materials, which find applications in optoelectronic, photovoltaic devices [1]. Among these materials,  $\text{In}_2\text{S}_3$  thin films appear to be promising candidates for many technological applications due to their stability and photoconductive behavior [2]. It can be used as an effective nontoxic substitute for cadmium sulfide (CdS) in thin film chalcogenide based solar cells. Even though CdS is capable of forming efficient heterojunction, there is great interest in replacing CdS by a cadmium-free buffer due to environmental reasons. We have already reported that  $\text{In}_2\text{S}_3$  buffer layer is quite efficient in yielding good results for ITO/CuInS<sub>2</sub>/ $\text{In}_2\text{S}_3$ /Ag thin film solar cell [3]. Cu(In,Ga)Se<sub>2</sub> based solar cell with  $\text{In}_2\text{S}_3$  buffer layer deposited by ALCVD could reach efficiencies (16.4%) near to those obtained by devices made with a standard CdS buffer layer [4]. Using sprayed  $\text{In}_x\text{S}_y$  buffer layer CIGS based solar cell could attain an efficiency of 8.9% [5].

Deposition of thin layer indium sulfide has been carried out by different methods such as MOCVD, spray pyrolysis, and chemical

bath deposition (CBD) [6–8] by several groups.  $\beta\text{-In}_2\text{S}_3$ , the stable phase of  $\text{In}_2\text{S}_3$  at room temperature, crystallizes in a defect spinel lattice, with a high degree of vacancies, ordering at tetrahedral cationic sites [9]. The characteristics of the film obtained depend highly on the fabrication method and can be changed by introducing dopants such as silver, tin, cobalt, aluminium etc. [10–14]. The primary purpose of our work was to decrease the resistance of  $\text{In}_2\text{S}_3$  layer, so that when it is used as buffer layer the reduced series resistance of the device will yield an increased short circuit current, and its verification on CZTS based solar cell.

The most efficient thin film solar cells currently use chalcogenides, such as Cu(In,Ga)(Se,S)<sub>2</sub> and CdTe as absorber layers giving laboratory efficiencies up to 20.3% [15] and 16.7% [16] respectively. Despite the promise, both technologies rely on elements that are scarce in the earth's crust. Currently immense research is going on to explore new alternative materials like AgInSe<sub>2</sub> [17,18] Cu<sub>2</sub>ZnSn(S,Se)<sub>4</sub> etc. Among them Cu<sub>2</sub>ZnSnS<sub>4</sub> is a promising absorber layer material with an absorption coefficient of  $10^4 \text{ cm}^{-1}$  and band gap energy in the range 1.4–1.6 eV [19–21]. Another key advantage is that CZTS can be synthesized by several economical techniques [22–25]. The highest conversion efficiency reported so far is 10.1% in a mixed sulfoselenide [Cu<sub>2</sub>ZnSn(S,Se)<sub>4</sub>] device [26] and 8.4% for the pure sulfide Cu<sub>2</sub>ZnSnS<sub>4</sub> device [27]. In the present work authors discuss the modification in the optoelectronic properties of  $\text{In}_2\text{S}_3$  buffer layer on indium diffusion and also the

\* Corresponding author. Tel.: +91 484 2577404; fax: +91 484 2577595.

E-mail addresses: [rajeshvgopinath@gmail.com](mailto:rajeshvgopinath@gmail.com) (V.G. Rajeshmon), [kpv@cusat.ac.in](mailto:kpv@cusat.ac.in) (K.P. Vijayakumar).

improvement in the performance parameters of a cell with this 'In' diffused  $\text{In}_2\text{S}_3$  as buffer layer and CZTS as absorber layer.

## 2. Experimental details

$\text{In}_2\text{S}_3$  thin films were deposited on soda lime glass (SLG) substrates using indigenously fabricated automated Chemical Spray Pyrolysis unit [20,28]. Aqueous solution containing indium chloride (0.03 M) and thiourea (0.3 M) is sprayed at a rate of 6 ml/min onto the substrate kept at 603 K using compressed air (pressure-1.5 bar) as the carrier gas. At the substrate surface, the spray droplets vaporize leaving a dry precipitate which instantly decomposes to form a thin layer of  $\text{In}_2\text{S}_3$ . Following deposition, films were annealed for 30 min at the substrate temperature. Concentration of thiourea was larger than the stoichiometric requirement to compensate for the loss of sulfur during pyrolysis. Out of the five films deposited (each having a thickness of 500 nm) four were taken and four different quantities of indium were evaporated. The thicknesses of the evaporated layers were 4, 6, 8, 10 nm (monitored using quartz-crystal thickness monitor attached to the vacuum evaporation unit) respectively. The films were then annealed at 100 °C for 1 h. Finally the samples were named as P:4In, P:6In, P:8In and P:10In respectively. The  $\text{In}_2\text{S}_3$  film devoid of indium evaporation was named as P. The crystal structure of the films was investigated using Rigaku (D. Max. C) X-ray diffractometer (employing  $\text{Cu-K}_\alpha$  line ( $\lambda = 1.5405 \text{ \AA}$ ) and Ni filter) operated at 30 kV and 20 mA. The observed XRD patterns were interpreted by comparing with the appropriate JCPDS cards. The depth wise variation of atomic concentration in the films was obtained using an X-ray photoelectron spectroscopy (XPS) ULVAC-PHI unit (Model-ESCA 5600 CIM) employing argon ion sputtering. Optical properties were studied using UV-vis-NIR spectrophotometer (Jasco V-570 Model). For Photoluminescence studies the samples were excited using the 325 nm output from a He-Cd laser and the emission was collected using CCD coupled spectrophotometer interfaced to the computer via custom made software OOLBase32. Electrical studies were conducted using Keithley 236 Source Measure Unit (SMU).

Glass plates coated with ITO (thickness 200 nm, optical transmission 82% and electrical resistivity  $2.25 \times 10^{-4} \Omega \text{ cm}$ ) were used as the substrate for junction fabrication. For depositing CZTS films, aqueous solution containing cuprous chloride (0.025 M), zinc acetate (0.01 M), stannic chloride (0.007 M) and thiourea (0.12 M) is sprayed at a rate of 6 ml/min onto the substrate kept at 623 K using compressed air (pressure ~ 1.5 bar) as the carrier gas. Concentration of thiourea was three times the stoichiometric requirement (0.04 M) to compensate for the loss of sulfur during pyrolysis. Thickness of CZTS layer was about 550 nm.  $\text{In}_2\text{S}_3$  layer of thickness 500 nm was deposited on top of CZTS layer. Five junctions were prepared using pristine as well as 'In' diffused  $\text{In}_2\text{S}_3$  layers and were named as D-P, D-P:4In, D-P:6In, D-P:8In and D-P:10In respectively. The  $J$ - $V$  characteristics of the devices were measured using the Keithley SMU K236 and Metric's Interactive Characterization Software (ICS). The devices were illuminated using a tungsten halogen lamp with an intensity of 100  $\text{mW/cm}^2$ , on the substrate surface. An infrared filter along with a water jacket was used to ensure that there was no heating of the device during measurement.

## 3. Results and discussion

### 3.1. X-ray diffraction studies

Fig. 1 shows the XRD pattern from  $10^\circ$  to  $60^\circ$  of pristine as well as indium diffused  $\text{In}_2\text{S}_3$  thin films. Well defined peaks corresponding to the (103), (109), (220) and (309) planes of  $\beta$ - $\text{In}_2\text{S}_3$  could be clearly observed. The 'd' values coincided with that of  $\beta$ - $\text{In}_2\text{S}_3$  in standard JCPDS data card (25–390). The intensity of peak corresponding to (220) plane was observed to be much greater than that of the other peaks present, indicating a strong preferential orientation in the (220) plane. For indium diffused samples, the Bragg peaks in the XRD pattern are more intense and the full width at half maximum (FWHM) of the diffraction peak is very small, indicating a clear improvement in crystallinity. However, it is also evident that there exists an optimum for the thickness of indium to be diffused, up to which the crystallinity increases and beyond which a retracing phenomenon is observed. For the 500 nm thick  $\text{In}_2\text{S}_3$  film studied here, the optimum thickness of indium to be diffused was 8 nm. The grain size was calculated (Table 1) from Debye-Scherrer formula,  $D = \frac{0.9\lambda}{\beta \cos \theta}$ , where  $D$  is the grain size,  $\lambda$  is the wavelength of  $\text{Cu-K}_\alpha$  line and  $\beta$  is the FWHM. Also no metallic phase was observed in the film in the detection limits of XRD analysis even for 10 nm 'In' diffused sample (P:10In). To investigate the effect of film thickness on the optimum quantity of indium to be diffused we

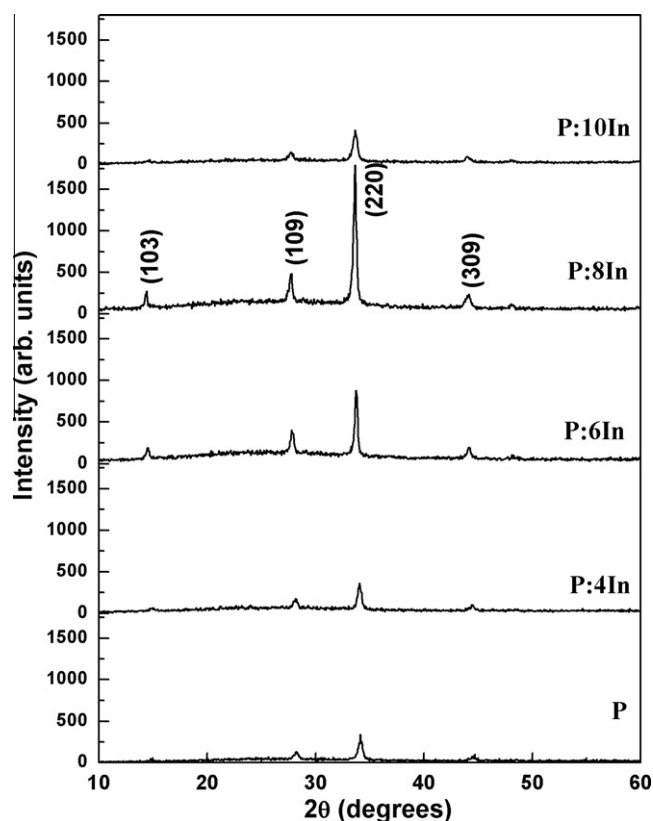


Fig. 1. X-ray diffraction patterns of pristine as well as 'In' diffused  $\text{In}_2\text{S}_3$  thin films prepared on SLG substrates.

Table 1

XRD data for pristine as well as 'In' diffused  $\text{In}_2\text{S}_3$  thin films.

Sample	d (Å)	Preferential orientation	FWHM (degrees)	Grain size (nm)
P	2.67	[220]	0.36	23.0
P:4In	2.67	[220]	0.35	23.7
P:6In	2.69	[220]	0.25	33.2
P:8In	2.70	[220]	0.24	34.5
P:10In	2.70	[220]	0.38	21.8
Standard JCPDS (25–390)	2.69	[220]	...	...

prepared  $\text{In}_2\text{S}_3$  films with thickness 600 nm. It was seen that the optimum thickness of indium diffused up to which crystallinity was enhanced increased from 8 to 9 nm with increase in thickness of  $\text{In}_2\text{S}_3$  film.

### 3.2. XPS studies

In order to confirm the formation of  $\text{In}_2\text{S}_3$  and to understand the variation of In/S ratio from surface to depth of the film on indium diffusion, XPS measurements were done. Fig. 2 shows the XPS depth profile of samples P and P:8In which indicates that indium and sulfur were uniformly distributed throughout the depth of the samples. Binding energies of indium and sulfur indicated the formation of  $\text{In}_2\text{S}_3$  (162.5 eV for  $\text{S}2p$ , 444.9 and 452.9 eV for  $\text{In } 3d_{5/2}$  and  $\text{In } 3d_{3/2}$  respectively) and were in agreement with the reported values [29]. Carbon was present as a surface contaminant (285 eV). Oxygen at the surface, which is found for all spray deposited samples, is due to surface contamination in the form of sulfite or sulfate. Oxygen content in the bulk of the sample is very low, but as we approach the substrate, it can be observed that oxygen

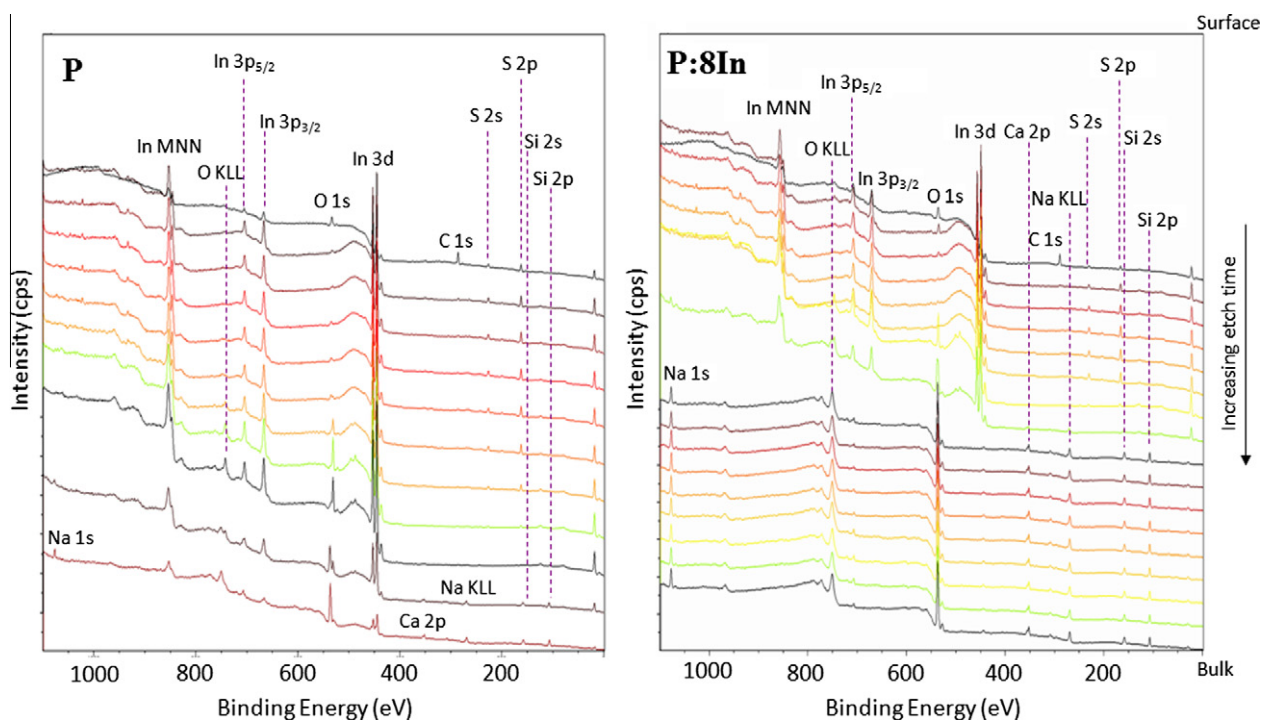


Fig. 2. XPS depth profile of samples P [pristine  $\text{In}_2\text{S}_3$  sample] and P:8In [ $\text{In}_2\text{S}_3$  sample in which 8 nm thick layer of 'In' is diffused].

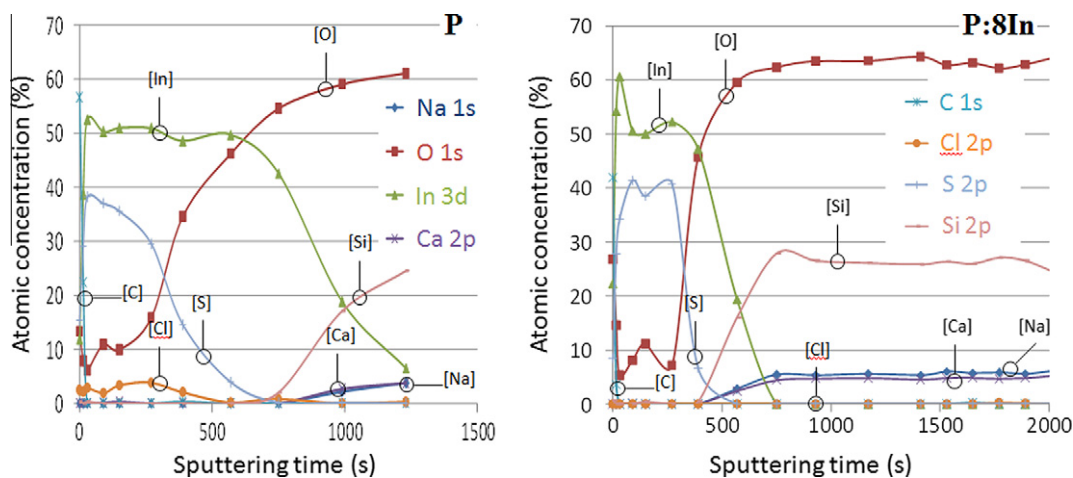


Fig. 3. Atomic concentration versus sputter time graph of elements obtained from X-ray photo electron spectroscopy for P [pristine  $\text{In}_2\text{S}_3$  sample] and P:8In [ $\text{In}_2\text{S}_3$  sample in which 8 nm thick layer of 'In' is diffused].

concentration is higher in the film towards the substrate side, due to diffusion of oxygen from glass to the film. The atomic concentration versus sputter time graph is shown in Fig. 3. Sputter time zero indicates the sample surface and as sputter time increases we get information from the depth. It can be seen clearly that in sample P:8In, 'In' concentration is high in a few surface layers when compared to sample P. 'In' concentration in the bulk is almost the same for both samples. The In/S ratio in the surface was calculated (from the area under the peak) for both samples and it was found that In/S ratio is 2.3 times higher in P:8In when compared to sample P.

### 3.3. Optical studies

Optical absorption spectra were recorded in the wavelength region 190–2500 nm. In order to determine the optical band gap,

$(\alpha h\nu)^2$  versus  $h\nu$  graph was plotted (Fig. 4). Optical band gap was determined from this plot for all films by applying linear fit to the straight line portion of the graph. Band gap of sample P was 2.64 eV which progressively decreased with increase in quantity of 'In' diffused and became 2.57 eV for P:8In. This shift in bandgap can be justified by the improved crystallinity of the samples with 'In' diffusion.

The PL spectrum of  $\text{In}_2\text{S}_3$  consists of two emission bands – a green emission centered at 540 nm and the red emission at 680 nm. The green emission is due to transition between donors created by vacancies of sulfur ( $V_s$ ) and acceptors due to vacancies of indium ( $V_{In}$ ). The red emission arises as a transition from indium interstitial ( $In_i$ ) donors to oxygen in vacancy of sulfur ( $O_{V_s}$ ) acceptors [30].  $\text{In}_2\text{S}_3$  is a material where two thirds of the lattice sites are vacant by birth itself [9]. When indium is diffused into  $\text{In}_2\text{S}_3$ , it

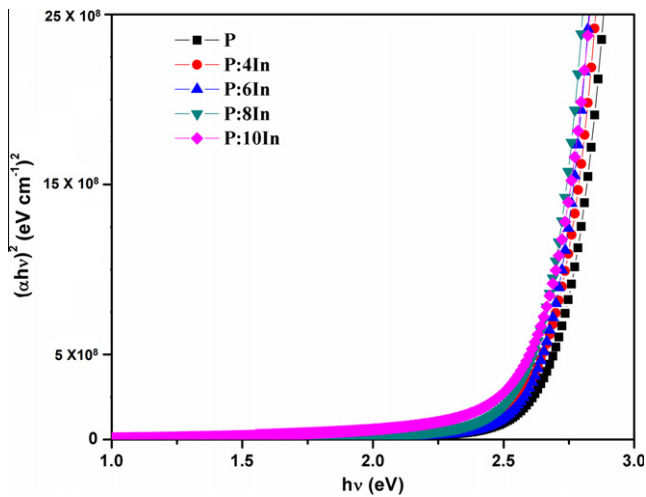


Fig. 4.  $(\alpha hv)^2$  versus  $h\nu$  plot for pristine and 'In' diffused  $\text{In}_2\text{S}_3$  films.

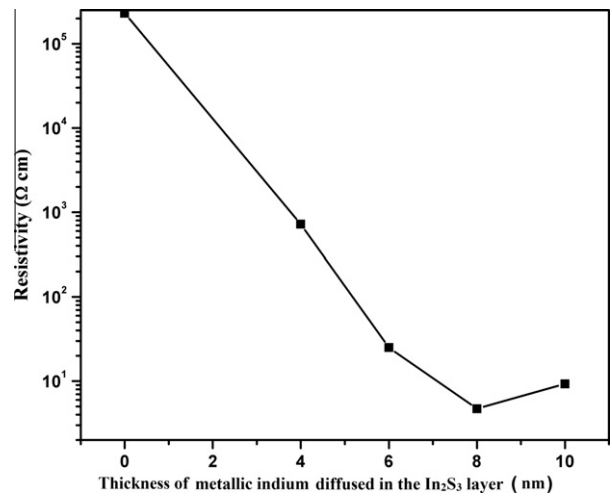


Fig. 6. Plot showing the variation of resistivity with 'In' diffusion.

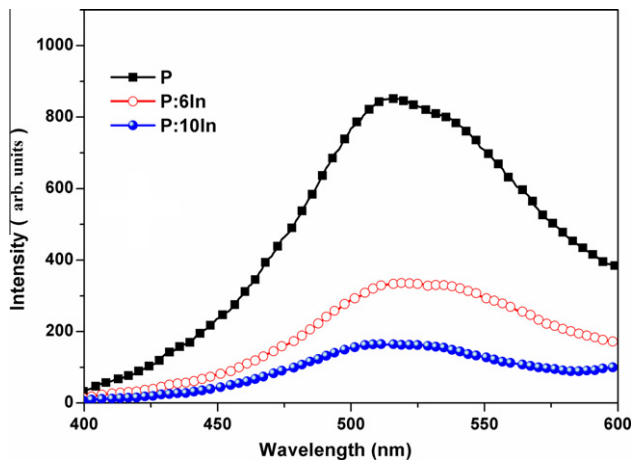


Fig. 5. Photoluminescence spectra of pristine as well as 'In' diffused  $\text{In}_2\text{S}_3$  films.

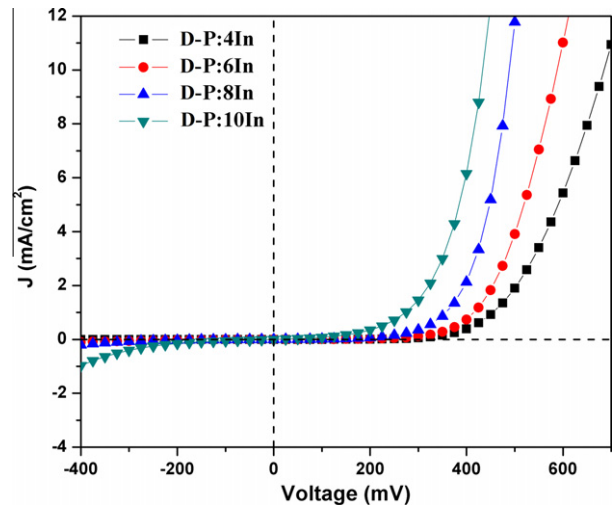


Fig. 7. Dark  $J$ - $V$  characteristics of the CZTS/ $\text{In}_2\text{S}_3$  heterojunctions fabricated with different amount of 'In' diffused into the buffer layer.

occupies the vacant cationic sites. Focusing mainly on the green emission in the PL spectrum (Fig. 5) of pristine as well as 'In' diffused  $\text{In}_2\text{S}_3$  samples; it can be observed that the intensity of green emission decreases as the quantity of 'In' diffused increases.

### 3.4. Electrical studies

Resistivity of samples was obtained using two probe measurements. For pristine sample resistivity was found to be  $2.3 \times 10^5 \Omega \text{ cm}$ . It reduced by five orders on indium diffusion and the variation in resistivity with the amount of 'In' diffused is shown in Fig. 6. From PL studies we observed a fall in the intensity of green emission which may be due to the decrease in concentration of defect centers  $V_{\text{In}}$  on indium diffusion. This might be the reason for reduction in resistivity of indium diffused  $\text{In}_2\text{S}_3$  thin films because scattering of carriers from defects will be reduced to a large extent. Resistivity of the samples was found to increase slightly beyond the optimum diffusion, which may be because the excess 'In' might be getting incorporated in interstitial positions, thereby increasing the resistance to the flow of carriers. 'In' diffusion was done with an aim to reduce resistivity and improve the crystallinity to ensure better carrier collection. Above studies clearly indicate that we could successfully accomplish our aim and to

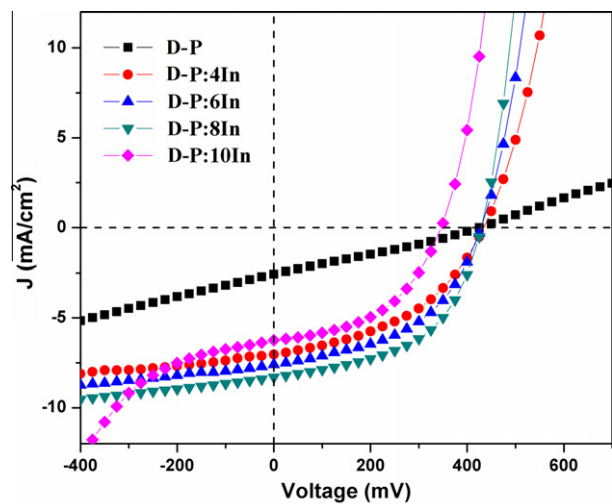


Fig. 8. Illuminated  $J$ - $V$  characteristics of the CZTS/ $\text{In}_2\text{S}_3$  heterojunctions fabricated with pristine and 'In' diffused buffer layer.

**Table 2**

A comparison of the photovoltaic parameters of the CZTS solar cells prepared using pristine as well as 'In' diffused Buffer layer.

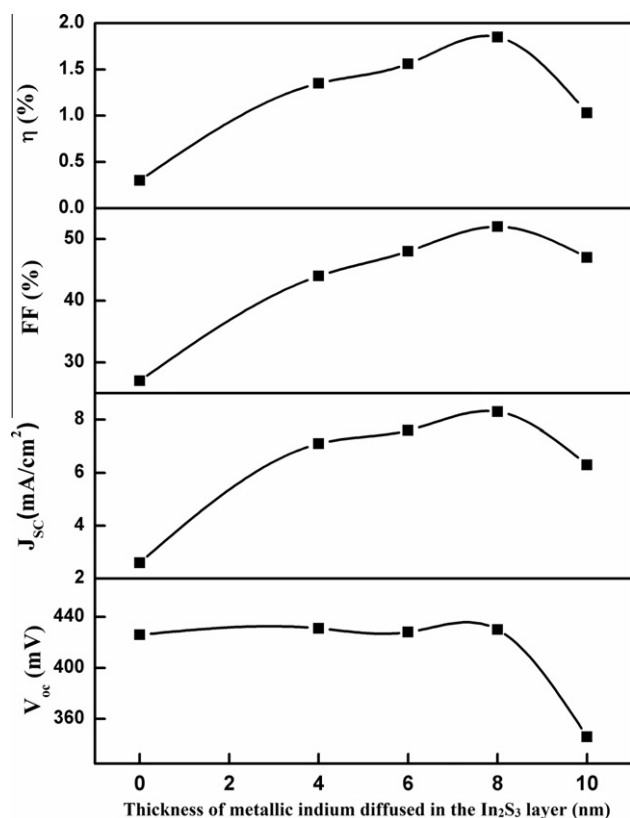
Device name	$V_{oc}$ (mV)	$J_{sc}$ (mA/cm <sup>2</sup> )	FF (%)	$\eta$ (%)	$R_s$ ( $\Omega$ cm <sup>2</sup> )	$R_{sh}$ ( $\Omega$ cm <sup>2</sup> )
D-P	426	2.6	27	0.30	114	170
D-P:4In	431	7.1	44	1.35	19.4	270
D-P:6In	428	7.6	48	1.56	13.4	236
D-P:8In	430	8.3	52	1.85	9.7	252
D-P:10In	346	6.3	47	1.03	13.3	222

confirm the results we fabricated devices with indium diffused  $In_2S_3$  as buffer layer.

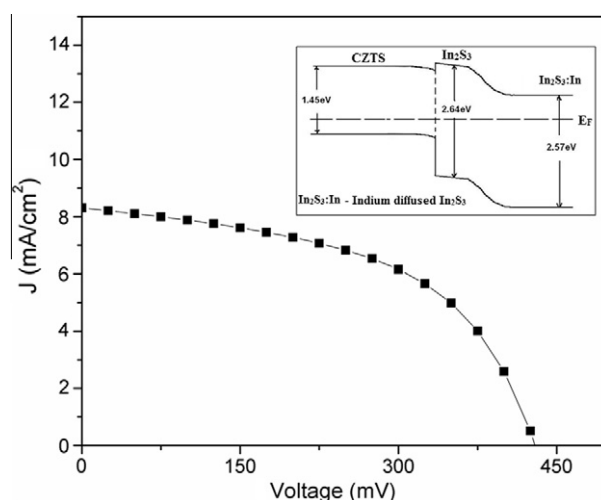
### 3.5. J–V characteristics of the CZTS/ $In_2S_3$ heterojunction with 'In' diffused buffer layer

Fig. 7 shows the dark J–V characteristics of the CZTS/ $In_2S_3$  heterojunction prepared using 'In' diffused  $In_2S_3$ . It could be observed that the knee voltage which is a measure of the junction voltage decreases with 'In' diffusion. As the amount of 'In' incorporated increases, it diffuses deeper, causing a reduction in high resistance region near the junction which thereby leads to a reduction in accumulation of charge and thus the knee voltage.

Short circuit current density of 2.7 mA/cm<sup>2</sup> and fill factor of 27% for the device prepared with pristine  $In_2S_3$  film is very low compared with devices fabricated with indium diffused buffer layer which is clearly evident from the illuminated J–V characteristics of the devices (Fig. 8). There is not much variation in the open-circuit voltage between devices except for D-P:10In. The more or less constant open circuit voltage for the other four devices may be because the diffused 'In' does not enter the junction region. In the case of D-P:10In, the quantity of diffused 'In' being higher, it enters



**Fig. 9.** Variation of  $V_{oc}$ ,  $J_{sc}$ , fill factor and  $\eta$  for CZTS/ $In_2S_3$  heterojunctions prepared with different quantities of indium diffused into the buffer layer.



**Fig. 10.** J–V characteristics of the best cell under illumination. Possible schematic of the band alignment between  $In_2S_3$  and CZTS is shown in the inset.

the junction and reduces the resistance. This in turn leads to larger leakage current (which is quite evident from the third quadrant of Fig. 8) and lower open circuit voltage. The short-circuit current density on the other hand increases steadily with increase in 'In' thickness up to the optimum value of 8 nm (i.e. up to D-P:8In) and then decreases. As the quantity of 'In' diffused is increased, the vacancies of indium (which are native defects) are filled, thereby reducing the resistivity of  $In_2S_3$  considerably and hence the increase in short circuit current density. The device fabricated using optimum 'In' diffused  $In_2S_3$  layer showed a fill factor of 52% and an efficiency of 1.85%. The performance parameters of all the devices fabricated have been tabulated in Table 2. Variation of  $V_{oc}$ ,  $J_{sc}$ , fill factor and  $\eta$  with different quantities of indium diffused in the buffer layer is depicted in Fig. 9. The buffer layer is modified in such a way that we achieve a high resistance region near the junction (intrinsic layer) which helps to produce a positive conduction band offset (CBO) and a low resistance region towards the contacts to enhance carrier collection. Using this we propose a possible band diagram for CZTS/ $In_2S_3$  junction as shown in the inset of Fig. 10. For calculating the exact position of Fermi level and for finding the value of CBO further studies using photo electron spectroscopy (PES) and inverse photoelectron spectroscopy (IPES) should be done.

### 4. Conclusions

The structural as well as electrical properties of  $In_2S_3$  thin films could be improved by 'In' diffusion. The properties were found to be the best for an optimum quantity of 'In' diffusion. The performance parameters of the CZTS/ $In_2S_3$  heterojunction could be significantly improved using 'In' diffused  $In_2S_3$  buffer layer. The device D-P:8In (fabricated using buffer layer with optimum quantity of 'In' diffused), showed a short circuit current density of 8.3 mA/cm<sup>2</sup>, open circuit voltage of 430 mV, fill factor of 52% and an efficiency of 1.85%.

### Acknowledgements

One of the authors [V.G.R.] would like to thank Council of Scientific and Industrial Research (CSIR) Govt. of India, for providing financial assistance. The authors are also thankful to the Department of Science & Technology, Govt. of India for providing financial support to initiate the works on automated spray system.

## References

- [1] K. Hara, K. Sayama, H. Arakawa, *Sol. Energy Mater. Sol. Cells* 62 (2000) 441.
- [2] L. Bhira, H. Essaidi, S. Belgacem, G. Couturier, J. Salardenne, N. Barreau, J.C. Bernede, *Phys. Status Solidi A* 181 (2000) 427.
- [3] T.T. John, M. Mathew, C. Sudha Kartha, K.P. Vijayakumar, T. Abe, Y. Kashiwaba, *Sol. Energy Mater. Sol. Cells* 89 (2005) 27.
- [4] N. Naghavi, S. Spiering, M. Powalla, B. Cavana, D. Lincot, *Prog. Photovolt. Res. Appl.* 11 (2003) 437.
- [5] K. Ernits, D. Bremaud, S. Buecheler, C.J. Hibberd, M. Kaelin, G. Khrypunov, U. Muller, E. Mellikov, A.N. Tiwari, *Thin Solid Films* 515 (2007) 6051.
- [6] R.S. Mane, C.D. Lokhande, *Mater. Chem. Phys.* 78 (2003) 15.
- [7] H. Spasevska, C.C. Kitts, C. Ancora, G. Ruani, *Int. J. Photoenergy* 2012 (2012) (Article ID 637943, 1).
- [8] O.A. Castelo-Gonzalez, H.C. Santacruz-Ortega, M.A. Quevedo-Lopez, M. Sotelo-Lerma, *J. Electron. Mater.* 41 (2012) 695.
- [9] K. Kambas, J. Spyridelis, M. Balkanski, *Phys. Status Solidi B* 105 (1981) 291.
- [10] M. Mathew, R. Jayakrishnan, P.M. Ratheeshkumar, C. Sudha Kartha, K.P. Vijayakumar, *J. Appl. Phys.* 100 (2006) 033504.
- [11] M. Kilani, C. Guasch, M. Castagne, N. Kamoun-Turki, *J. Mater. Sci.* 47 (2012) 3198.
- [12] W.T. Kim, W.S. Lee, C.S. Chung, C.D. Kim, *J. Appl. Phys.* 63 (1988) 5472.
- [13] N. Kamoun, S. Belgacem, M. Amlouk, R. Bennaceur, J. Bonnet, F. Touhari, M. Nouaoura, L. Lassabatere, *J. Appl. Phys.* 89 (2001) 2766.
- [14] M. Mathew, M. Gopinath, C. Sudha Kartha, K.P. Vijayakumar, Y. Kashiwaba, T. Abe, *Sol. Energy* 84 (2010) 888.
- [15] P. Jackson, D. Hariskos, E. Lotter, S. Paetel, R. Wuerz, R. Menner, W. Wischmann, M. Powalla, *Prog. Photovolt. Res. Appl.* 19 (2011) 894.
- [16] M.A. Green, K. Emery, Y. Hishikawa, W. Warta, *Prog. Photovolt. Res. Appl.* 18 (2010) 346.
- [17] F.A. Al-Agel, Waleed E. Mahmoud, *Mater. Lett.* 82 (2012) 82.
- [18] H. Mustafa, D. Hunter, A.K. Pradhan, U.N. Roy, Y. Cui, A. Burger, *Thin Solid Films* 515 (2007) 7001.
- [19] W. Darenfed, M.S. Aida, N. Attaf, J. Bougdira, H. Rinnert, *J. Alloys Comp.* 542 (2012) 22.
- [20] V.G. Rajeshmon, C. Sudha Kartha, K.P. Vijayakumar, C. Sanjeeviraja, T. Abe, Y. Kashiwaba, *Sol. Energy* 85 (2011) 249.
- [21] A.V. Maholkar, S.S. Shinde, A.R. Babar, K.U. Sim, H.K. Lee, K.Y. Rajpure, P.S. Patil, C.H. Bhosale, J.H. Kim, *J. Alloys Comp.* 509 (2011) 7439.
- [22] A. Wangperawong, J.S. King, S.M. Herron, B.P. Tran, K. Pangan-Okimoto, S.F. Bent, *Thin Solid Films* 519 (2011) 2488.
- [23] M. Patel, I. Mukhopadhyay, A. Ray, *J. Phys. D: Appl. Phys.* 45 (2012) 445103.
- [24] Y. Wang, H. Gong, *J. Alloys Comp.* 509 (2011) 9627.
- [25] M. Cao, Y. Shen, *J. Crystal Growth* 318 (2011) 1117.
- [26] D. Aaron, R. Barkhouse, Oki Gunawan, Tayfun Gokmen, Teodor K. Todorov, David B. Mitzi, *Prog. Photovolt. Res. Appl.* 20 (2012) 6.
- [27] Byungha Shin, Oki Gunawan, Yu Zhu, Nestor A. Bojarczuk, S. Jay Chey, Supratic Guha, *Prog. Photovolt. Res. Appl.* (2012), <http://dx.doi.org/10.1002/pip.1174> (Short Commun.).
- [28] T. Sebastain, M. Gopinath, C. Sudha Kartha, K.P. Vijayakumar, T. Abe, Y. Kashiwaba, *Sol. Energy* 83 (2009) 1683.
- [29] T.T. John, S. Bini, Y. Kashiwaba, T. Abe, Y. Yasuhiro, C. Sudha Kartha, K.P. Vijayakumar, *Semicond. Sci. Technol.* 18 (2003) 491.
- [30] R. Jayakrishnan, T. Sebastian, C. Sudha Kartha, K.P. Vijayakumar, *J. Appl. Phys.* 111 (2012) 093714.